Frequency response analysis of photodiodes for optical communications

J. M. TORRES PEREIRA
Instituto de Telecomunicações, Department of Electrical and Computer Engineering, Instituto Superior Técnico, Av. Rovisco Pais, 1049-001 Lisboa, Portugal

This paper presents in detail the computed results regarding the effect of the absorption layer width, bias voltage, temperature, wavelength and direction of the incident light on the transit time limited frequency response of photodiodes for optical communications. The simulation model is quite general and may be applied to photodiodes with an arbitrary electric field profile and non-uniform illumination. The results were obtained for *p-i-n* structures with an absorption layer of $In_{0.53}Ga_{0.47}As$ and they show that better bandwidths may be obtained for shorter devices, lower temperature and, when the light incident on the p^+ side, for shorter wavelengths.

(Received May 27, 2010; accepted July 14, 2010)

Keywords: Modelling, Frequency response, Photodiode, P-i-n, Temperature

1. Introduction

Photodiodes are widely used in optical communication systems because they can easily be fabricated and have good frequency response [1]. For the 1.0-1.6 m wavelength range the basic device consists of a *p-i-n* heterostructure with absorption region of $In_{0.53}Ga_{0.47}As$ and doped regions of lattice matched InP [2].

The frequency response of *p-i-n* photodiodes may determine the performance of the optical communication system and therefore it is important to study in detail its dependence on the device's structural and operating parameters. The frequency response of *p-i-n* photodiodes has been investigated using several numerical techniques under various assumptions [3-5]. Analytical solutions may be obtained when the carriers' drift velocities in the absorption region are assumed to be constant which, in general, is not the case for long devices and/or small reverse bias voltages. For an arbitrary electric field profile the frequency response has been computed very accurately by considering that the absorption region is divided into an adequate number of layers where the electric field, and therefore the drift velocity of electrons and holes, is constant [6].The calculation of the frequency response for this multilayer structure is based on the response of each layer using matrix algebra [7].

In this paper a very comprehensive account of the effect of the absorption layer width, bias voltage, temperature, wavelength and direction of the incident light on the transit time limited frequency response of *p-i-n* photodiodes is presented.

2. Device structure and modelling

The *p-i-n* structure under study is shown in Fig. 1. The contact layers are of highly *p* and *n* doped InP semiconductor. Between the contacts there is an absorption layer of lightly *n* doped $In_{0.53}Ga_{0.47}As$.

The light may be incident from either side of the device however, for the wavelength range under investigation, the optical absorption is only significant in the ternary semiconductor. The photodiode is assumed to be reverse biased and the bias voltages are high enough to deplete the whole absorption region. In this case the resulting electric field extends throughout the absorption region and is responsible for the transport of the optical generated electrons and holes.

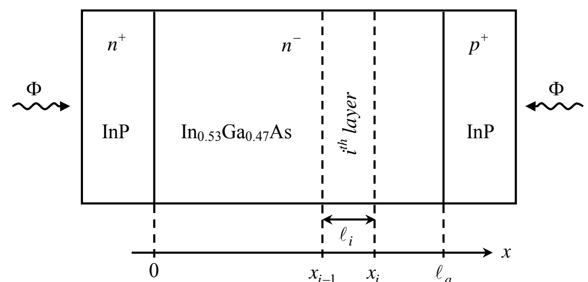

Fig. 1. Schematic of the p-i-n structure used in this work. The light (Φ) may be incident on the p^+ side or on the n^+ side.

The numerical model used to compute the frequency response of *p-i-n* photodiodes has been presented elsewhere and it will be described briefly in the following paragraphs [6].

The absorption region is first divided into a certain number of layers where the electric field is assumed to be constant. The continuity equations are then solved for each layer, with analytical solutions for the electron and hole current densities. Each layer may then be characterized by four linear response coefficients which, by following a simple set of rules, can be combined to give the

coefficients for the whole structure. The device's frequency response is derived from these coefficients. This staircase approximation of the electric field in the absorption region enables us to obtain the device's frequency response with the required accuracy for any electric field profile, by the proper choice of the size and number of layers.

In the frequency domain the continuity equations for electrons and holes in the ith layer may be written as:

$$\frac{i\omega}{v_{in}} J_{in}(x,\omega) = \frac{d\,J_{in}(x,\omega)}{dx} + G_i(x,\omega) \quad (1)$$

$$\frac{i\omega}{v_{ip}} J_{ip}(x,\omega) = -\frac{d\,J_{ip}(x,\omega)}{dx} + G_i(x,\omega) \quad (2)$$

where $J_{in}(x,\omega)$ and $J_{ip}(x,\omega)$ are the electron and hole current densities respectively, v_{in}, v_{ip} are the electron and hole drift velocities respectively and $G_i(x,\omega)$ refers to the electron-hole generation rate due to optical absorption in the ith layer which, for light incident on the n^+-side, is given by

$$G_i(x,\omega) = q\alpha\phi_1 e^{-\alpha x} \quad \left(x_{i-1} \le x \le x_i\right) \quad (3)$$

and , for light incident on the p^+-side, is given by

$$G_i(x,\omega) = q\alpha\phi_1 e^{-\alpha(\ell_a - x)} \quad \left(x_{i-1} \le x \le x_i\right) \quad (4)$$

The parameter α is the absorption coefficient, q is the magnitude of the electron charge and ϕ_1 is the amplitude of the sinusoidal input optical flux component.

The ith layer may then be represented by a set of linear response coefficients $T_i, \vec{S}_i, \vec{R}_i$ and D_i. The coefficients $T_i, \vec{S}_i$ are related to the electron and hole current densities through the equations

$$\begin{bmatrix} J_{ip}(x_i) \\ J_{in}(x_i) \end{bmatrix} = T_i \begin{bmatrix} J_{ip}(x_{i-1}) \\ J_{in}(x_{i-1}) \end{bmatrix} + \vec{S}_i \quad (5)$$

with

$$T_i = \begin{bmatrix} T_{ipp} & T_{ipn} \\ T_{inp} & T_{inn} \end{bmatrix} \quad and \quad \vec{S}_i = \begin{bmatrix} S_{ip} \\ S_{in} \end{bmatrix} \quad (6)$$

The coefficients $\vec{R}_i$ and D_i are obtained from the equation

$$p_i(\omega) = \vec{R}_i^T \begin{bmatrix} J_{ip}(x_{i-1}) \\ J_{in}(x_{i-1}) \end{bmatrix} + D_i \quad (7)$$

being

$$p_i(\omega) = \int_{\ell_i} \left[J_{in}(x,\omega) + J_{ip}(x,\omega)\right] dx \quad (8)$$

The coefficient D_i is a scalar whereas $\vec{R}_i^T = \left[R_{ip} \quad R_{in}\right]$.

The frequency response $I(\omega)$ may then be expressed as:

$$I(\omega) = (D - R_n S_n)/(T_{nn}\ell_a) \quad (9)$$

where D, R_n, S_n, T_{nn} are quantities derived from the coefficients for the whole structure which may be obtained following a simple set of rules

$$\begin{aligned} T_{i+1,i} &= T_{i+1} T_i \\ \vec{S}_{i+1,i} &= \vec{S}_{i+1} + T_{i+1}\vec{S}_i \\ \vec{R}_{i+1,i}^T &= \vec{R}_{i+1}^T T_i + \vec{R}_i^T \\ D_{i+1,i} &= \vec{R}_{i+1}^T \vec{S}_i + D_{i+1} + D_i \end{aligned} \quad (10)$$

with subscripts (i), $(i+1)$ and $(i+1,i)$ referring to the ith layer, $(i+1)^{th}$ layer and the union of the two layers respectively.

For the ith layer and light incident on the n^+-side, $T_i, \vec{S}_i, \vec{R}_i$ and D_i are given by:

$$T_i = \begin{bmatrix} e^{-i\omega\tau_{ip}} & 0 \\ 0 & e^{i\omega\tau_{in}} \end{bmatrix} \qquad \vec{R}_i = \ell_i \begin{bmatrix} f\left(i\omega\tau_{ip}\right) \\ f\left(-i\omega\tau_{in}\right) \end{bmatrix} \quad (11)$$

$$\vec{S}_i = q\alpha\phi_1\ell_i \; e^{-\alpha x_i} \begin{bmatrix} f\left(i\omega\tau_{ip} - \alpha\ell_i\right) \\ -f\left(-i\omega\tau_{in} - \alpha\ell_i\right) \end{bmatrix} \quad (12)$$

$$D_i = q\alpha\phi_1\ell_i^2 e^{\alpha(\ell_i - x_i)} \left[\frac{f\left(\alpha\ell_i\right) - f\left(-i\omega\tau_{in}\right)}{\alpha\ell_i + i\omega\tau_{in}} - \frac{f\left(\alpha\ell_i\right) - f\left(i\omega\tau_{ip}\right)}{\alpha\ell_i - i\omega\tau_{ip}}\right] \quad (13)$$

with $\tau_{ip} = \ell_i / v_{ip}, \tau_{in} = \ell_i / v_{in}$ being the hole and electron transit time in the ith layer respectively and $f(\theta) = (1 - e^{-\theta})/\theta$. When the light is incident on the p^+-side the expressions for T_i and $\vec{R}_i$ do not change but $\vec{S}_i$ and D_i are given by [8]

$$\vec{S}_i = q\alpha\phi_1\ell_i \; e^{-\alpha(\ell_a - x_i)} \begin{bmatrix} f\left(i\omega\tau_{ip} + \alpha\ell_i\right) \\ -f\left(-i\omega\tau_{in} + \alpha\ell_i\right) \end{bmatrix} \quad (14)$$

$$D_i = q\alpha\phi_1\ell_i^2 e^{-\alpha\ell_a} e^{-\alpha(\ell_i - x_i)} \left[\frac{f\left(-\alpha\ell_i\right) - f\left(-i\omega\tau_{in}\right)}{-\alpha\ell_i + i\omega\tau_{in}} + \frac{f\left(-\alpha\ell_i\right) - f\left(i\omega\tau_{ip}\right)}{\alpha\ell_i + i\omega\tau_{ip}}\right] \quad (15)$$

The electric field in the absorption region may be approximated by [9]

$$E(x) = \frac{2U_d}{\ell_a^2} x + \left(\frac{U - U_d}{\ell_a}\right) \quad (U > U_d) \quad (16)$$

with U the reverse bias voltage and U_d the punchthrough voltage given by $U_d = \frac{qN\ell_a^2}{2\varepsilon_n}$, where N is the residual donor concentration in the absorption region and ε_n its dielectric constant.

The electron and hole drift velocities in the $In_{0.53}Ga_{0.47}As$ are calculated, for each value of the electric field, from two empirical expressions that show very good agreement with experimental results [4]:

$$\begin{aligned} v_n(E) &= \left(\mu_n E + \beta v_{n\ell} E^{\gamma}\right) / \left(1 + \beta E^{\gamma}\right) \\ v_p(E) &= v_{p\ell} \tanh\left(\mu_p E / v_{p\ell}\right) \end{aligned} \tag{17}$$

with μ_n, μ_p the electron and hole mobilities respectively and $v_{n\ell}$, v_{pl} the electron and hole saturation drift velocities respectively; β = 7.4x10^{-15} (m/V)$^{2.5}$; γ =2.5.

The temperature affects the drift velocities because the mobilities and the saturation drift velocities change with temperature. For the InGaAs we consider that, at T= 300 K, μ_n= 1.05 m^{2}V^{-1}s^{-1} and μ_p= 0.042 m^{2}V^{-1}s^{-1} and that, for the range of temperatures under consideration, $\mu \propto T^{-1}$ [10]. The saturation drift velocities may be related to the absolute temperature by [10]

$$\begin{aligned} v_{n\ell} &= 7.7\text{x}10^4 - 53T \quad \text{(m/s)} \\ v_{p\ell} &= 6.59\text{x}10^4 - 53.4T \quad \text{(m/s)} \end{aligned} \tag{18}$$

The drift velocity for electrons and holes as a function of the electric field, at T= 273 K, 300 K and 350 K, is shown in Fig. 2. An increase of temperature is seen to decrease the drift velocity, the effect being more important for the electrons at low electric fields.

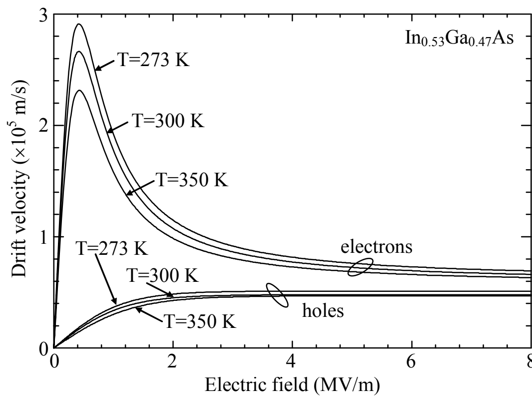

Fig. 2. Electron and hole drift velocity versus electric field for $In_{0.53}Ga_{0.47}As$ at several temperatures.

The absorption coefficient depends on temperature mainly due to changes in the energy band gap, W_G. For $In_{0.53}Ga_{0.47}As$ it may be expressed as

$$\alpha(T) = \alpha(300)\sqrt{\frac{hf - W_G(T)}{hf - W_G(300)}} \tag{19}$$

with hf representing the energy of the incident optical radiation and $W_G(T)$ given by [2]

$$\begin{aligned} W_G(T) = 0.812 - 3.26\text{x}10^{-4}T + \\ + 3.31\text{x}10^{-7}T^2 \quad \text{(eV)} \end{aligned} \tag{20}$$

The absorption coefficient also depends on the wavelength of the incident radiation which, for T = 300K and λ in μm, may be given by [11]:

$$\alpha(\lambda) = \exp(3.935 - 3.524\lambda + 0.47\lambda^2)\ \text{x}10^6 \ \ (\text{m}^{-1}) \tag{21}$$

and is represented in Fig. 3 for T= 273 K and 350 K. The absorption coefficient decreases when the wavelength increases and the temperature decreases. From Fig. 3 it is clear that the absorption coefficient is more sensitive to the wavelength than to the temperature.

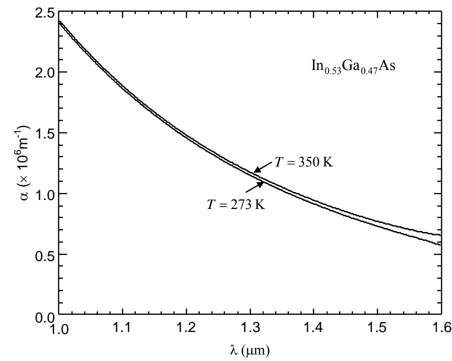

Fig. 3. The absorption coefficient versus wavelength for $In_{0.53}Ga_{0.47}As$ at several temperatures.

3. Results and discussion

The p-i-n structure under study is assumed to have an absorption region of n-type lightly doped $In_{0.57}Ga_{0.43}As$ with impurity concentration N= 10^{21}m^{-3}. The light is assumed to be incident on the p^+ side unless stated otherwise. The calculations were based on absorption regions divided into 10 equally spaced layers because the results did not differ from those obtained with 100 or more layers [6].

Fig. 4 shows the computed frequency response of p-i-n photodiodes at T= 300 K and λ= 1.55 μm for ℓ_a = 1.5 μm and 3 μm and U= 6 V and 10 V. These results show that the frequency response is more sensitive to the absorption region width than to the bias voltage. Better frequency response is obtained for shorter devices, which is related to the decrease of the carriers' transit time. A slight increase of the frequency response for lower voltages may be explained in terms of the drift velocity-electric field type of dependence for the electrons which, for incidence on the p^+ side, are the dominant carriers. For

incidence on the n^+ side the holes are the dominant carriers and, for the same reasons, the results should be reversed as it has already been reported [8]. The fact that the electrons have higher drift velocities than the holes also explains why the frequency response is better for incidence on the p^+ side [8].

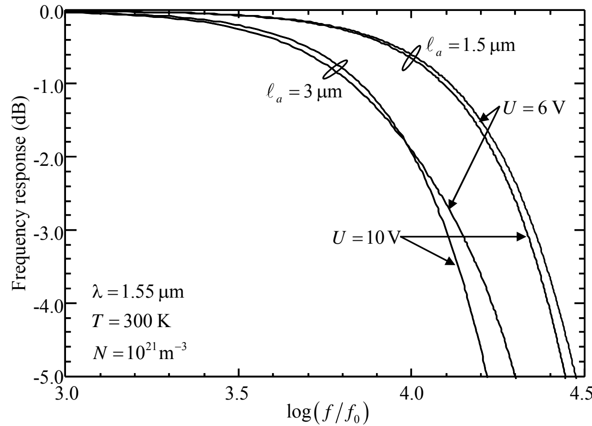

Fig. 4. Computed frequency response of p-i-n photodiodes at T= 300 K and λ= 1.55 μm for ℓ_a = 1.5 μm and 3 μm and U= 6 V and 10 V (f_0 = 1 MHz).

The computed frequency response of a *p-i-n* photodiode with ℓ_a = 3 μm and *U*= 6 V for *T*= 300 K and 350 K and λ= 1.0 μm and 1.55 μm is shown in Fig. 5. For a fixed temperature long wavelength optical radiation is seen to give worse frequency response, which agrees with other published results [3]. When the wavelength increases the absorption coefficient decreases, i.e., light is absorbed deeper into the absorption region. For light incident on the p^+ side the observed results may be explained in terms of an increasing contribution of holes to the photocurrent, which have lower drift velocity than the electrons. The frequency response is also seen to improve when the temperature decreases. These results indicate that the effect of temperature is more important on the drift velocity than on the absorption coefficient.

The effect of the width of the absorption region on the bandwidth for *T*= 300 K and 350 K and U= 6 V and 10 V is shown in Fig. 6, when λ= 1.3 μm. The bandwidth decreases about 8 GHz when the absorption region width increases from 1.5 μm to 3.0 μm. When the temperature increases from 300 K to 350 K the bandwidth decreases more than 1 GHz for *U*= 6 V and less than 1 GHz for *U*= 10 V. The bandwidth is about 2 GHz and 3 GHz higher for *U*= 6 V than for *U*= 10 V when ℓ_a= 1.5 and 3.0 μm respectively. Shorter devices at lower bias voltages have larger bandwidths. However they are more sensitive to temperature.

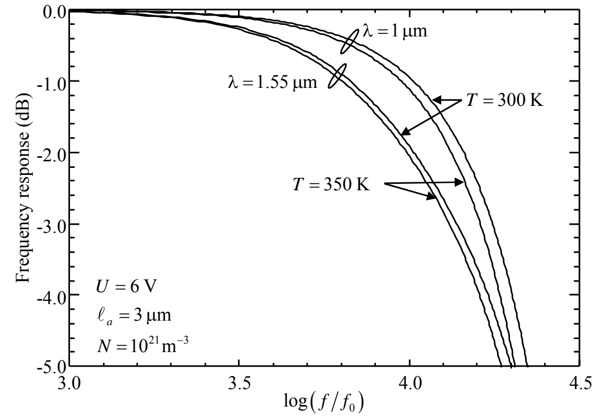

Fig. 5. Computed frequency response of a p-i-n photodiode with ℓ_a = 3 μm and U= 6 V for T= 300 K and 350 K and λ= 1.0 μm and 1.55 μm (f_0 = 1 MHz).

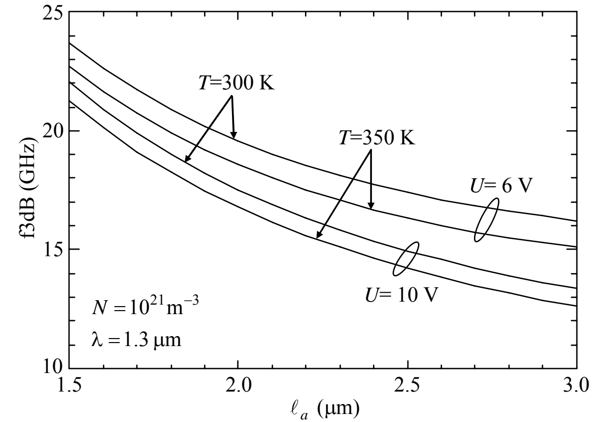

Fig. 6. Computed bandwidth of a p-i-n photodiode as a function of the absorption layer width for T= 300 K and 350 K and U= 6 V and 10 V, λ= 1.3 μm.

Fig. 7 shows the bandwidth dependence on ℓ_a, for several values of the wavelength at *T*=300 K and *U*= 6V, when the light is incident on the n^+ or p^+ side. The best bandwidth values are obtained for light incident on the p^+ side. For incidence on the p^+ side the bandwidth is seen to decrease when the wavelength increases, the effect being more important for longer devices. However, as predicted, if the light is incident on the n^+ side an increase of the bandwidth is observed when the wavelength increases. For λ= 1.55 μm, the bandwidth is about 4 GHz and 8 GHz higher when light is incident on the p^+ side than when light is incident on the n^+ side, for ℓ_a= 1.5 μm and 3.0 μm respectively.

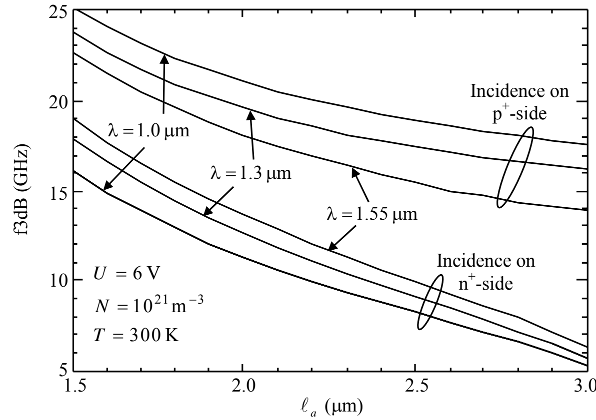

Fig. 7. Computed bandwidth of a p-i-n photodiode as a function of the absorption layer width at T= 300 K and U= 6 V, for λ= 1.0 μm, 1.3 μm and 1.55 μm and light incident on the p^+ or on the n^+ side.

For long devices, ℓ_a = 3 μm, and *U*= 10 V the bandwidth does not seem to change for the wavelength range of 1.0-1.2 μm, Fig. 8, because optical generation takes place mostly in the absorption region close to the p^+ contact.

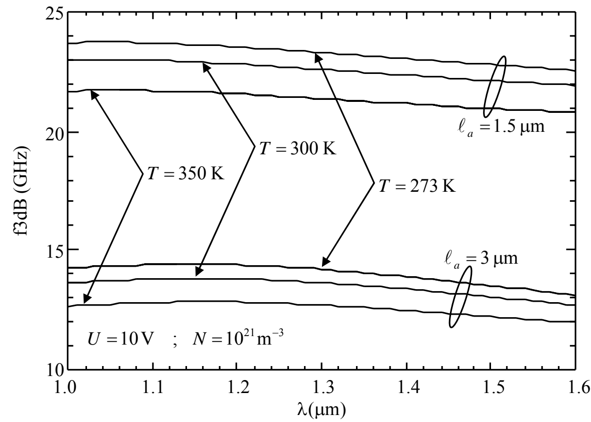

Fig. 8. Computed bandwidth of a p-i-n photodiode as a function of wavelength when U= 10 V for T= 273 K, 300 K and 350 K and ℓ_a = 1.5 μm and 3 μm.

For longer wavelengths the increasing contribution of holes to the photocurrent is responsible for the observed decrease in the bandwidth. The wavelength range, for which the bandwidth saturation is observed, decreases when the bias voltage decreases, Fig. 9. Devices biased at *U*= 6 V seem to be more sensitive to changes in the absorption coefficient than those biased at *U*= 10 V, which may be due to the electron drift mobility-electric field type of dependence.

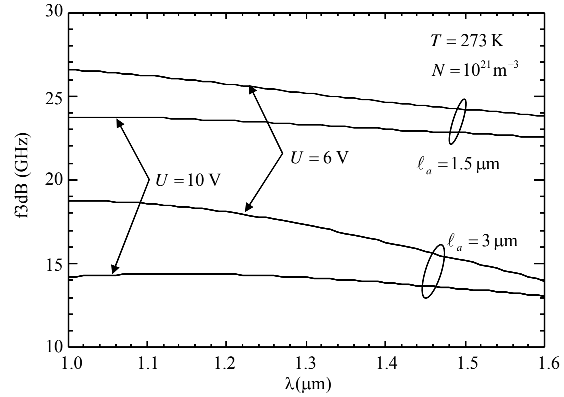

Fig. 9. Computed bandwidth of a p-i-n photodiode as a function of wavelength at T= 273 K for U= 6 V and 10 V and ℓ_a = 1.5 μm and 3 μm.

The bandwidth as a function of temperature is shown in Fig. 10, for devices biased at *U*= 6 V with ℓ_a = 1.5 μm and 3.0 μm at λ= 1.3 μm and 1.55 μm. When the temperature increases from 273 K to 350 K the bandwidth decreases about 2 GHz. For a fixed temperature and low bias voltage longer devices seem to be more sensitive to wavelength changes than shorter devices.

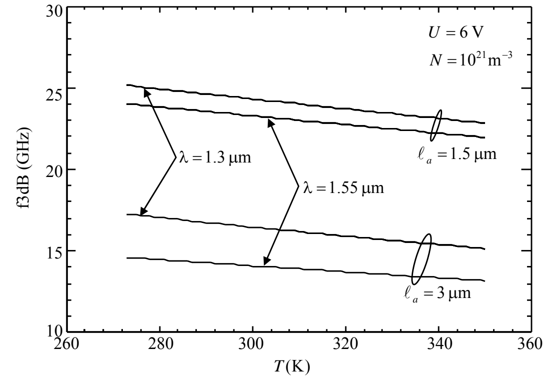

Fig. 10. Computed bandwidth of a p-i-n photodiode as a function of temperature when U= 6 V for λ= 1.3 μm and 1.55 μm and ℓ_a = 1.5 μm and 3 μm.

4. Conclusions

This paper investigates the effect of the absorption region width, bias voltage, temperature and wavelength on the transit time limited frequency response of InP/InGaAs/InP *p-i-n* photodiodes. In this simulation model, valid for an arbitrary electric field profile and non-uniform illumination, the absorption region is divided into a certain number of layers where the electric field is assumed to be constant. Each layer may then be represented by a set of linear response coefficients that can be combined, by a simple set of rules, to give the linear response coefficients for the multilayer structure which are then used to obtain the device's frequency response. The

bandwidth of *p-i-n* photodiodes is strongly dependent on the absorption region width due to its effect on the carriers' transit time. An increase of the absorption region width increases the carriers' transit time and therefore decreases the bandwidth. An increase of temperature is seen to decrease the drift velocity and increase the absorption coefficient. The reported decrease of bandwidth, when the temperature increases, shows that the effect of temperature is more important on the drift velocities than on the absorption coefficient. The device's bandwidth is higher for light incident on the p^+ side than for light incident on the n^+ side. For light incident on the p^+ side, the bandwidth increases when the wavelength decreases because the photocurrent is mostly determined by the optical generated electrons. However, if the light is incident on the n^+ side, the bandwidth increases when the wavelength increases due to an increasing contribution of electrons to the photocurrent. The bias voltage also affects the device's bandwidth due to the drift velocity-electric field type of relationship for electrons and holes in the absorption region. For light incident on the p^+ side lower bias voltages give better bandwidths however they seem to be more sensitive to temperature and wavelength changes.

Acknowledgments

This work was supported by Instituto de Telecomunicações – pólo de Lisboa, under the project P186.

References

[1] M. Makiuchi, H. Hamaguchi, T. Mikawa, O. Wada, IEEE Photon. Technol. Lett. **3**, 530 (1991).
[2] T. P. Pearsall, IEEE J. Quantum Electron. **QE-16**, 709 (1980).
[3] G. Lucovsky, R. F. Schwarz, R. B. Emmons, J. Appl. Phys. **35**, 622 (1964).
[4] M. Dentan, B. de Cremoux, J. Lightwave Technol. **8**, 1137 (1990).
[5] R. Sabella, S. Merli, IEEE J. Quantum Electron. **29**, 906 (1993).
[6] J. M. T. Pereira, COMPEL **26**, 1114 (2007).
[7] J. N. Hollenhorst, J. Lightwave Technol. **8**, 531 (1990)
[8] J. M. T. Pereira, in Studies in Appl Electromagnetics and Mechanics 30 - Advanced Computer Techniques in Applied Electromagnetics, edited by S. Wiak et al., IOS Press 2008.
[9] J. B. Radunovic, D. M. Gvozdic, IEEE Trans. Electron. Dev. **40**, 1238 (1993).
[10] S. Adachi, Physical Properties of III-V Semiconductor Compounds, Wiley, 1992.
[11] J. A. Jervase, H. Bourdoucen, IEEE Trans. Electron. Dev. **47**, 1158 (2000).

*Corresponding author: torres.pereira@lx.it.pt